

Contents lists available at ScienceDirect

# **Toxicology Letters**

journal homepage: www.elsevier.com/locate/toxlet



# A study on the in vitro percutaneous absorption of silver nanoparticles in combination with aluminum chloride, methyl paraben or di-n-butyl phthalate



Katarzyna Domeradzka-Gajda<sup>a</sup>, Marek Nocuń<sup>a</sup>, Joanna Roszak<sup>a</sup>, Beata Janasik<sup>a</sup>, C. Derrick Quarles Jr.<sup>d</sup>, Wojciech Wąsowicz<sup>a</sup>, Jarosław Grobelny<sup>b</sup>, Emilia Tomaszewska<sup>b</sup>, Grzegorz Celichowski<sup>b</sup>, Katarzyna Ranoszek-Soliwoda<sup>b</sup>, Małgorzata Cieślak<sup>c</sup>, Dorota Puchowicz<sup>c</sup>, Jhanis J. Gonzalez<sup>d</sup>, Richard E. Russo<sup>d</sup>, Maciej Stępnik<sup>a,\*</sup>

- a Department of Toxicology and Carcinogenesis, Nofer Institute of Occupational Medicine, Łódź, Poland
- <sup>b</sup> Department of Materials Technology and Chemistry, University of Łódź, Łódź, Poland
- <sup>C</sup>Scientific Department of Unconventional Technologies and Textiles, Textile Research Institute, Łódź, Poland
- d Applied Spectra, Inc., Fremont, CA, USA

#### HIGHLIGHTS

- · Citrate, PEG stabilized silver nanoparticles minimally penetrate pig skin in vitro.
- · Aluminum chloride, methyl paraben, butyl phthalate do not modify the penetration.
- · Laser ablation-ICP-MS is a useful technique for studying skin sections.

#### ARTICLE INFO

Article history: Received 26 October 2016 Received in revised form 6 March 2017 Accepted 8 March 2017 Available online 14 March 2017

Keywords: Silver nanoparticles Percutaneous absorption Aluminum Methyl paraben Di-n-butyl phthalate Laser ablation ICP-MS

#### ABSTRACT

Some reports indicate that the silver released from dermally applied products containing silver nanoparticles (AgNP) (e.g., wound dressings or cosmetics) can penetrate the skin, particularly if damaged. AgNP were also shown to have cytotoxic and genotoxic activity. In the present study percutaneous absorption of AgNP of two different nominal sizes (Ag15 nm or Ag45 nm by STEM) and surface modification, i.e. citrate or PEG stabilized nanoparticles, in combination with cosmetic ingredients, i.e. aluminum chloride (AlCl<sub>3</sub>), methyl paraben (MPB), or di-n-butyl phthalate (DBPH) was assessed using in vitro model based on dermatomed pig skin.

The inductively coupled plasma mass spectrometry (ICP-MS) measurements after 24 h in receptor fluid indicated low, but detectable silver absorption and no statistically significant differences in the penetration between the 4 types of AgNP studied at 47, 470 or 750  $\mu$ g/ml. Similarly, no significant differences were observed for silver penetration when the AgNP were used in combinations with AlCl<sub>3</sub> (500  $\mu$ M), MPB (1250  $\mu$ M) or DBPH (35  $\mu$ M). The measured highest amount of Ag that penetrated was 0.45 ng/cm<sup>2</sup> (0.365–0.974 ng/cm<sup>2</sup>) for PEG stabilized Ag15 nm + MPB.

© 2017 Elsevier B.V. All rights reserved.

#### 1. Introduction

Wide application of nanomaterials in skin cosmetics raises reasonable questions about consumer safety. There is an ongoing

E-mail address: mstep@imp.lodz.pl (M. Stępnik).

debate on capability of nanomaterials to penetrate through the skin. Some reports indicate such possibility, particularly through damaged skin. Quantum dots QD-565 and QD-655 have been shown to penetrate into the dermis of abraded rat skin (Zhang and Monteiro-Riviere, 2008). Peptide-functionalized fullerenes translocated to the intercellular space of the stratum granulosum layer of flexed but not to unflexed excised porcine skin (Rouse et al., 2007).

<sup>\*</sup> Corresponding author at: Nofer Institute of Occupational Medicine, 8 Sw. Teresy St., Łódź, Poland.

Silver nanoparticles (AgNP) are the most popular advertised nanomaterial present in 438 of the 1814 (24%) products listed in the Nanotechnology Consumer Product Inventory (Vance et al., 2015). Very comprehensive database on products containing nanomaterials, updated daily, "The Nanodatabase" (http:// nanodb.dk/en/search-database) currently lists 2601 nanoproducts of which 400 are registered as nanosilver containing products (accessed on 2017.02.21). The products are from different categories: health and fitness, cosmetics, personal care, or even food, beverage supplements, cooking. Another inventory maintained by two European consumer organizations. ANEC/BEUC (http://www.beuc.eu/safety/nanotechnology; accessed 2017.02.21) lists nanosilver containing products which come in contact with the skin, like cleansers, crèmes, moisturizers, antiperspirants, washing lotions, soaps, foot balms or shoe deodorants. The majority of AgNP applications results from their strong antibacterial properties (Durán et al., 2015a) primarily linked to release of silver ions.

Available literature data on percutaneous absorption of AgNP mainly concerns studies with medical products, like dressings containing AgNP used to treat wounds, burns, and scars. Some reports strongly indicate that the silver released from these products can penetrate the skin, particularly if damaged (Vlachou et al., 2007; Wang et al., 2009; Moiemen et al., 2011; Pfurtscheller et al., 2014). The studies on percutaneous absorption through normal skin provide evidence for small but detectable penetration of silver nanoparticles (Larese et al., 2009; Bianco et al., 2014, 2015). When nanosilver dressings were applied to healthy patients with normal intact skin approximately 5 days prior to surgery, AgNP penetrated intact skin and could be identified as deep as the reticular dermis (George et al., 2014). Zhu et al. (2015) using surface-enhanced Raman scattering (SERS) microscopy observed that the penetration depth of poly-N-vinylpyrrolidone AgNP dispersed in pure water exceeded the stratum corneum (SC) thickness of porcine ear, however it was not clear if it was due to penetration of trace amounts of AgNP through the SC barrier or the silver presence inside the hair follicles.

As the cosmetics are usually mixtures of many ingredients, there is a possibility of modification of percutaneuous absorption of AgNP by the ingredients. This question becomes more relevant when some of the formulations are applied on micro-abraded skin, like underarm roll-on deodorants or antiperspirants, where the region of the skin may be regularly shaved. For example, it is not known how the presence of aluminum salts in antiperspirants can influence AgNP absorption. Many effective antiperspirants currently available on the market such as NIVEA, Dove or AXE contain aluminum salts (e.g. aluminum chloride, chlorohydrate or aluminum zirconium tetrachlorohydrex gly) at concentrations reaching 20%. Similarly, no data is available on a potential modification of AgNP absorption by other popular cosmetic ingredients, like parabens or phthalates. Although, cosmetic companies try to diminish content of parabens in their products, many formulations applied on skin still contain one or more of them. For example, NIVEA uses parabens in around 30% of its products (https://www. nivea.co.uk/advice/nice-skin/parabens-in-cosmetics), primarily in body care, sun protection and face care products. Methyl paraben (MPB) is the most frequently used antimicrobial preservative (Soni et al., 2002) and shows the highest solubility in water compared to other parabens. According to the Scientific Committee on Consumer Safety (SCCS), MPB used as preservative in cosmetics at the maximum authorized concentrations (0.4% for one ester or 0.8% when used in combination) is considered safe for human health (SCCS, 2010, 2013). Phthalates have been banned in the European Union under the Cosmetics Directive as CMR substances, however they are allowed as traces and/or impurities, not used intentionally in the perfumes at up to 100 ppm total or per

substance (SCCP, 2007). Dibutyl phthalate (DBPH) was found in a variety of consumer products (Koniecki et al., 2011).

As in the open literature there is no information on potential influence of different cosmetic ingredients on percutaneous absorption of AgNP, in the present study we conducted a series of such measurements using in vitro model based on isolated pig skin. Porcine skin is a very good model representing penetration of human skin because it has thickness and absorption rates comparable to those of human skin (Monteiro-Riviere and Riviere, 1996). We used AgNP of different nominal size (15 nm or 45 nm) and surface modification, i.e. citrate or PEG stabilized nanoparticles, in combination with aluminum chloride (AlCl<sub>3</sub>), methyl paraben (MPB), or dibutyl phthalate (DBPH). For detection of silver in different matrices (receptor fluid and histopathological skin sections) powerful techniques based on ICP-MS and laser ablation ICP-MS were applied (Becker et al., 2014).

#### 2. Materials and methods

#### 2.1. Chemicals and reagents

Nitric acid (65%, pure P.A. #529603115) was purchased from POCH (Poland). Aluminum chloride (AlCl<sub>3</sub>, #06220), methyl paraben (MPB, #H6654), di-n-butyl phthalate (DBPH, #524980), Nile Red (#72485), 4',6-diamidino-2-phenylindole dihydrochloride (DAPI, #32670), MTT (3-(4,5-dimethylthiazol-2-yl)-2,5-diphenyl-tetrazolium bromide #M5655), Hanks' Balanced Salt Solution (HBSS without phenol red, pH 7.4, #H9269: KCl 0.4, KH<sub>2</sub>PO<sub>4</sub> 0.06, NaCl 8.0, NaHCO<sub>3</sub> 0.35, Na<sub>2</sub>HPO<sub>4</sub> 0.04788 g/L) were from Sigma-Aldrich, Co.

Silver nitrate (AgNO<sub>3</sub>, 99.999% metals basis), PEG [poly(ethylene glycol) methyl ether thiol, Mw=6000] were purchased from Aldrich. Sodium citrate ( $C_6H_5Na_3O_7$ ·2 $H_2O$ ,  $\geq$ 99%) was bought from Sigma–Aldrich. Tannic acid ( $C_{76}H_{52}O_{46}$ , pure), sodium borohydride (NaBH<sub>4</sub>,  $\geq$ 99%) were purchased from Fluka.

2.2. Synthesis and physico-chemical characterization of silver nanoparticles

#### 2.2.1. Citrate stabilized Ag 45 nm

#### 2.2.1.1. Citrate stabilized Ag 45 nm colloid synthesis.

To the aqueous solution of silver nitrate (94.5 g, 0.017 wt%), stirred and heated to the boiling point under reflux, a warm mixture of tannic acid (1.3 g, 5 wt%) and sodium citrate (4.2 g 1 wt%) was added. After a few seconds the solution colored to brown (formation of AgNP). The mixture was stirred for additional 15 min under reflux and next cooled down to room temperature. The silver colloid was stored in darkness. The concentration of silver was 100 ppm.

#### 2.2.1.2. Citrate stabilized Ag 45 nm colloid purification.

The synthesized colloid was purified to remove tannins by centrifugation (three times; rotation centrifugal force RCF = 18,944 g; 30 min). Twice removed supernatant was replaced with the aqueous solution of sodium citrate (0.03 wt%). In the last step of centrifugation the supernatant was removed and the colloid was concentrated to 750 ppm (concentration determined by the atomic adsorption spectroscopy (AAS); silver nanoparticles solubilized with 70% of nitric acid before measurement). Before the AAS measurements the colloid was filtered through a 0.1 µm polyvinylidene fluoride (PVDF) membrane. The final concentration of sodium citrate and tannic acid in the colloid was 2950 ppm and 8 ppm, respectively.

### 2.2.2. PEG stabilized Ag 45 nm

AgNP were synthesized according to procedure described in citrate stabilized Ag 45 nm colloid synthesis. AgNP with the size of about 45 nm were modified with PEG-ligand [poly(ethylene glycol) methyl ether thiol, Mw=6000]. Briefly, the modification of NPs was carried out during the colloid purification stage (double centrifugation and next removed supernatant was replaced with deionized water). After the first step of purification process the colloid was modified with PEG ligand. The amount of PEG used for modification corresponds to 10 ligand molecules per  $1\,\mathrm{nm}^2$  of NP surface (shape of NPs – spherical; size of NPs – 45 nm; NPs concentration – 100 ppm). After the modification the colloid was left for 24 h. Next, the colloid was purified by double centrifugation (RCF=18,944 g, 30 min) from the excess of unbound PEG-ligand and concentrated to 750 ppm. After the first centrifugation the supernatant was replaced with deionized water and after the second centrifugation the supernatant was removed. In the next step the colloid was filtered through a 0.1  $\mu\mathrm{m}$  polyvinylidene fluoride (PVDF) membrane. The final

concentration of sodium citrate and tannic acid in colloid was: 10 ppm and 8 ppm respectively. The final concentration of silver in colloid was 750 ppm (determined by the atomic adsorption spectroscopy; silver nanoparticles solubilized with 70% of nitric acid before measurement).

#### 2.2.3. Citrate stabilized Ag 15 nm

AgNP with the size of about 15 nm were synthesized according to seed growth mediated method on AgNP seeds with the size of about 6 nm.

#### 2.2.3.1. Synthesis of Ag seeds.

Silver seeds with the size of about 6 nm used for the synthesis of 15 nm AgNP were prepared according to chemical reduction method. Briefly, to the 94.5 g of aqueous solution of silver nitrate (0.016 wt%) a mixture of sodium citrate (4.2 g, 4 wt%) and tannic acid (0.63 g, 5 wt%) was added. After about 10 s 0.7 g of an aqueous solution of sodium borohydride (2 wt%) was incorporated to the reaction solution. The mixture was stirred for 15 min and after the synthesis process stored in darkness. The size of silver seeds was determined based on the dynamic light scattering (DLS) and scanning transmission electron microscopy (STEM) techniques. AgNP with the mean size of about 6 nm were used as seeds to obtain AgNP with the size of about 15 nm.

#### 2,2,3.2. Citrate stabilized Ag 15 nm colloid synthesis.

A mixture of 5.7 g of seeds colloid, 4.1 g of sodium citrate (4 wt%) and 39.2 g of deionized water was stirred and warmed to the boiling point. Next, to the boiling mixture an aqueous solution of silver nitrate (16 ml, 0.122 wt%) was incorporated using a capillary and infusion pump (10 ml h $^{-1}$ ). After the silver nitrate introduction the solution was stirred for additional 5 min and next cooled down to room temperature. The final concentration of AgNP in colloid was 200 ppm.

#### 2.2.3.3. Citrate stabilized Ag 15 nm colloid purification,

The AgNP citrate colloid was purified to remove tannins by double centrifugation (RCF=18,944 g, 30 min). In the first step the removed supernatant was replaced by the aqueous solution of sodium citrate (0.03 wt%) and in the second the supernatant was removed the colloid was concentrated to 1000 ppm (concentration determined with AAS; silver nanoparticles solubilized with 70% of nitric acid before measurement). Before the AAS measurements the colloid was filtered through a 0.1 µm polyvinylidene fluoride (PVDF) membrane. The final concentration of sodium citrate and tannic acid in colloid was 2950 ppm and 5 ppm, respectively. By the dilution with the aqueous solution of sodium citrate (0.03 wt%) the final concentration of Ag colloid was adjusted to 750 ppm (as in the case of Ag 45 nm).

#### 2.2.4. PEG stabilized Ag 15 nm

AgNP were synthesized according to procedure described in citrate stabilized Ag 15 nm colloid synthesis. The modification and purification of Ag 15 nm with PEG-ligand [poly(ethylene glycol) methyl ether thiol, Mw=6000] was performed according to the procedure already described in PEG stabilized Ag 45 nm. The amount of PEG used for modification corresponds to 10 ligand molecules per 1 nm² of NP surface (shape of NPs – spherical; size of NPs – 15 nm; NPs concentration – 200 ppm). The colloid was filtered through a 0.1  $\mu$ m polyvinylidene fluoride (PVDF) membrane. The final concentration of sodium citrate and tannic acid in colloid was: 750 ppm (measured with atomic adsorption spectroscopy, silver nanoparticles solubilized with 70% of nitric acid before measurement).

#### 2.2.5. Physical characterization

AgNP were characterized using UV-vis spectroscopy, dynamic light scattering (DLS) and scanning transmission electron microscopy (STEM). The UV-vis spectra were recorded with a spectrophotometer USB2000+ detector (miniature fiber optic spectrometer), Ocean Optics, HL-2000 (tungsten halogen light sources) using 1 cm quartz cuvette. STEM measurements were performed by scanning electron microscope (Nova NanoSEM 450, FEI, accelerating voltage of 30 kV). Samples for STEM investigations were prepared as follows: a drop of colloid was deposited onto carbon-coated copper grids (300 mesh). The suspension was left for 2 h for solvent evaporation. The size distribution histogram was obtained based on the selection of at least 500 NPs.

# 2.3. DLS measurements of AgNP colloid and suspensions of AgNP in combinations with AlCl $_3$ , MPB, DBPH

Dynamic light scattering (DLS) was carried out on a Malvern Zetasizer Nano ZS instrument (25 °C, laser wavelength 633 nm; cuvette; polycarbonate DTS 1070 cells,

Malvern). The scattering was monitored at a fixed angle of 173° in backward scattering mode. The data were derived from the correlation function of the scattered intensity as a number-weighed size distribution. Size distribution analysis was performed using an NNLS-type algorithm. DLS measurements of synthesized AgNP colloid were performed at medium viscosity 0.887 mPa-s, material refractive index 1.330. Stock AgNP colloid was diluted with Hanks' Balanced Salt Solution (HBSS) to the desired concentration. After vortexing, 10  $\mu$ l of stock solution of AlCl<sub>3</sub> (50 mM) in distilled water, 10  $\mu$ l of MPB (125 mM) or DBPH (3.5 mM) in DMSO was added to 990  $\mu$ l of the freshly prepared AgNP colloid.

#### 2.4. Franz<sup>TM</sup> diffusion cells

The jacketed clear glass cells (%11.28~mm, i.e.  $1~\text{cm}^2$ ) with a flat flange joint and a 5 ml receptor volume were used (#4G-01-00-11.28-05, SES GmbH-Analysesysteme, Bechenheim, Germany). All glassware was first washed with 65% HNO $_3$  solution and then soaked overnight in diluted HNO $_3$  at 4% (v/v) with Milli-Q water. Next, they were rinsed five times with Milli-Q water. The cells were placed in a Franz-cell holder equipped with magnetic stirrer/heater circulator with thermostat system (Model V9-CB-02, SES GmbH-Analysesysteme) (Fig. S1 in Supplementary Information). In each experiment the test preparations were run using 3 Franz cells.

#### 2.5. Preparation of the split-thickness skin

The pig skin samples were procured from ears of animals from a slaughterhouse. The samples were cleaned and immediately frozen after isolation. After transportation to the laboratory the samples were stored at  $-20\,^{\circ}\mathrm{C}$  until analysis (usually within 1 month). Before the percutaneous studies, the skin samples were thawed at RT, washed with 70% ethanol, dried, shaved, and the top layer including epidermis with dermis (~400  $\mu$ m) was cut off using a Schink dermatome 12".

Quality control of skin thickness was performed for each sample before mounting on a diffusion cell using a digital high-precision micro caliper with a resolution of 0.01 mm. Additionally, randomly selected skin disks were fixed in 10% formalin, ethanol dehydrated, paraffin embedded and processed for routine histopathological examination. Skin section thickness was assessed using images collected in at least 5 fields per slide using software provided with Leica TCS SP8 confocal microscope.

Additionally, during validation of the method and thereafter before the experiments, MTT reduction test was performed to check for metabolic activity of the skin disks. To this end, representative disks of the same size were prepared using cork bore  $\Phi10$  mm and then incubated with MTT solution in HBSS (0.5 mg/ml) for 3 h at 37 °C. Afterwards, the disks were washed in HBSS and incubated overnight in  $500\,\mu l$  of acidified isopropanol at  $4\,^{\circ}C$  to extract the blue formazan. The optical density of the extracts ( $100\,\mu l$ ) was measured using a Multiscan RC spectrophotometer (Labsystems Helsinki, Finland) with a  $550\,\mathrm{nm}$  filter and  $620\,\mathrm{nm}$  filter as a reference.

#### 2.6. Measurements of percutaneous absorption of silver nanoparticles in combination with test chemicals (AlCl<sub>3</sub>, MPB, DBPH)

In the study, the option of an infinite dose (hence the worst case scenario) was selected. In this option resembling the underarm conditions, the concentration of test substance in the donor compartment is not significantly diminished during the study and the maximum absorption rate is achieved. Each piece of trimmed skin disk was clamped between the donor and the receptor compartment. The skin was allowed to equilibrate with the receptor fluid for 30 min before substance application.

In the first part of the study, the transdermal penetration was assessed for 3 concentrations of AgNP: 750 μg/ml, i.e. neat colloidal AgNP suspension; 470 μg/ml, i.e. AgNP 1.6imes diluted in HBSS; or 47  $\mu$ g/ml, i.e. AgNP 16imes diluted in HBSS. The donor part of the skin was incubated with 100 µ.l/cm<sup>2</sup> of an AgNP suspension. For the second part of the study, the AgNP concentration of 470  $\mu g/ml$  was selected, and used in combinations of the test chemicals at possibly their highest final concentrations resulting from limits of solubility in aqueous medium (HBSS), i.e. AlCI<sub>3</sub> at 0.5 mM, MPB at 1.25 mM, and DBPH at 0.035 mM. Control cells were incubated with a mixture of HBSS and the solution used for AgNP preparation (1:1, v/v). The receptor compartment was filled with HBSS, and kept to maintain the epidermal surface temperature at  $36 \pm 1$  °C in order to reproduce the underarm physiological temperature at normal conditions. The temperature of the receptor compartment was maintained by a magnetic stirring bar. Samples of the receptor fluid (1 ml) were withdrawn from the sampling port after 24 h. During the experiment the donor compartment was sealed with Parafilm "M". The experiments were performed once or twice, always in triplicates per test preparation. The separate experiments were performed using skin samples taken from different animals.

#### 2.6.1. Fluorescent staining of skin sections

After the exposure the skin disks were washed of excess test preparations and fixed in 10% neutral buffered formalin solution and subsequently embedded in paraffin, according to standard procedures. Sections (5  $\mu$ m) after rehydration were

stained with Nile Red (NR) (for nonpolar lipids) and DAPI (for DNA) for general morphological assessment. Stock solutions of NR (1 mg/ml in acetone) and DAPI (1 mg/ml in DMSO) were prepared and stored at  $-20\,^{\circ}\text{C}$ . A fresh NR/DAPI staining solution was prepared by adding 10  $\mu\text{I}$  of stock NR solution and 10  $\mu\text{I}$  of stock DAPI solution to 1 ml of 75% glycerol, followed by vortexing. A drop of staining solution was added to the sections. After 10 min at room temperature in darkness, the sections were rinsed in distilled water. The sections were visualized using Leica TCS SP8 confocal microscope.

#### 2.7. Determination of silver content in receptor fluid by ICP-MS

A PerkinElmer Elan Elan DRC-e inductively coupled plasma mass spectrometer (ICP-MS) was used for silver determination. The sample introduction system consisted of a quartz cyclonic spray chamber, Mainhard nebulizer and a peristaltic four-channel pump, Calibration standard solution were prepared from 10 mg/L multi-element calibration standard 3 (PerkinElmer Pure Plus) by proper dilution with ultrapure water. A NIST reference material (1643e) was used to determine the method accuracy. Data acquisition was performed in triplicate measurements for each sample, and deionized (DI) water was analyzed between replicates to check memory effects.

#### 2.8. Analysis of skin samples by LA-ICP-MS

To conduct the analysis, the skin disks after 24 h exposure in the Franz chambers were washed of excess test preparations, fixed in 10% neutral buffered formalin solution, embedded in paraffin and sectioned at 20  $\mu m$ .

An Applied Spectra, Inc. (ASI, Fremont, CA) J200 Laser Ablation (LA) instrument equipped with a Nd:YAG 266 nm nanosecond laser was used in combination with a Bruker Aurora Elite ICP-MS. The laser was set for a repetition rate of 10 Hz, a 35  $_{\rm min}$  laser spot size (diameter), and 0.38 mJ per laser pulse. A gas purged chamber was used at 0.7 L/min helium carrier gas and 0.7 L/min argon make-up gas. Each skin cross section was sampled in parallel line mode, with line scan spacing of 0.07 mm, and the sample stage was translated at 0.1 mm/s. Each parallel line had a delay of 30 seconds, which was optimized for the data analysis software. The area ablated was never larger than  $\sim$ 14.0 mm in width  $x\sim$ 4.0 mm in height. The ICP-MS was set to 1400 W (RF), 18.0 L/min argon gas (coolant), 0.8 L/min argon gas (auxiliary), sheath gas flow of 0.8 L/min argon. Isotopes  $^{12}$ C,  $^{31}$ P,  $^{34}$ S, and  $^{107}$ Ag were measured using a dwell time of 8 ms in peak hopping mode. All LA-ICP-MS data was analyzed

and converted into 2D elemental images using Applied Spectra, Inc.'s Data Analysis Software.

#### 2.8.1. Preparation of calibration curves

A solution used to prepare nanoparticle suspensions was used as the blank for the Ag nanoparticle calibration curves. Two stock solutions of silver nanoparticles, Ag 15 nm at 750  $\mu$ g/ml and Ag45 at 750  $\mu$ g/ml, were used to create the calibration standards. Calibration standards were prepared at concentrations of 5, 50, 100, 250, 470, and 750  $\mu$ g/ml. These calibration standards were mixed well, placed onto a paraffin block, and allowed to dry before analysis. Three replicate areas (1 mm²) were ablated using the same conditions as aforementioned from each silver nanoparticle standard dried on paraffin (Fig. S2 in Supplementary Information).

#### 2.9. Statistical analysis

Silver concentration data (mg/ml) in the receptor solution were converted to the total amount that penetrated the skin (mg/cm²). All results are presented as median 25–75 percentile. The difference between independent groups was assessed using the Kruskal–Wallis test, A p value <0.05 was considered as the limit of statistical significance. The calculations were performed using Statistica v8.0 (StatSoft. Inc., USA).

#### 3. Results

#### 3.1. Physico-chemical characterization

The synthesized (citrate stabilized NP) and modified with PEGligand AgNP were characterized with DLS and UV-vis techniques (Fig. 1). Moreover, the size of the metallic core of citrate stabilized AgNP was determined with the STEM technique which was crucial for calculation of PEG-ligand amount required for modification process.

Citrate stabilized Ag samples exhibited the maximum of the absorption band at  $408\,\mathrm{nm}$  and  $423\,\mathrm{nm}$ ; i.e. in the region

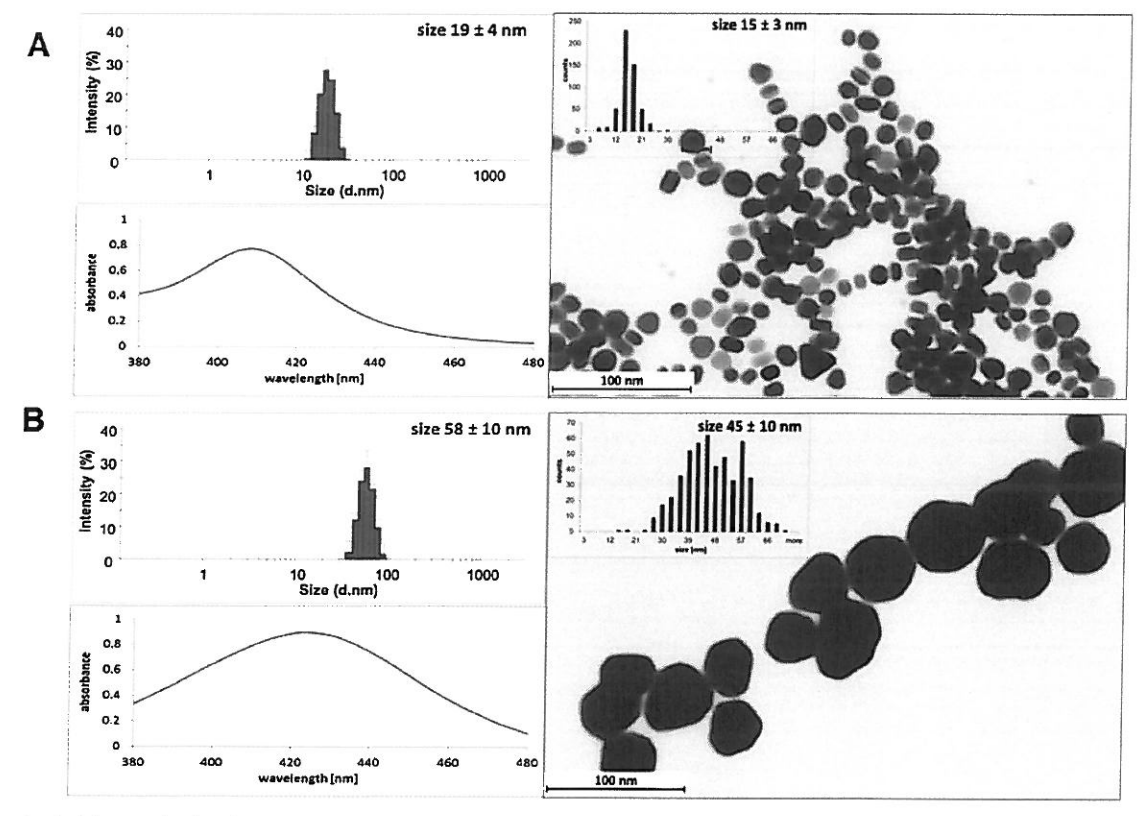


Fig. 1. Physicochemical characterization of citrate stabilized silver nanoparticles. DLS size distribution graphs, UV-vis spectra and scanning transmission electron microscopy (STEM) images with size distribution histograms of the silver nanoparticles. A. Sample 1-15 nm, B. Sample 2-45 nm.

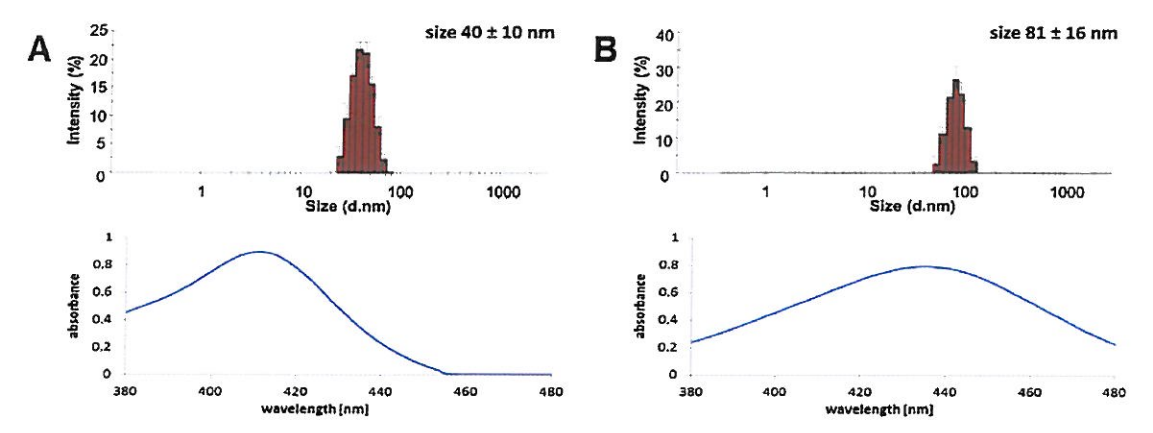


Fig. 2. Physicochemical characterization of PEG stabilized silver nanoparticles. DLS size distribution graphs and UV-vis spectra of the silver nanoparticles. A. Sample 3-15 nm, B. Sample 4-45 nm.

characteristic for particles smaller than 20 nm (sample 1) and for particles with the size about 50 nm (sample 2). The mean size of metallic core of citrate stabilized Ag was  $15\pm3$  nm and  $45\pm10$  nm for sample 1 and 2, respectively. The hydrodynamic size of particles was  $19\pm4$  nm and  $58\pm10$  nm. Any aggregates or agglomerates were not observed in both cases.

The effectiveness of surface modification was monitored with DLS and UV–vis techniques (Fig. 2). The size of metallic core of AgNP investigated with STEM technique remained unchanged after the modification process with PEG (data not shown). However, after the modification process with PEG-ligand, the hydrodynamic size of AgNP increased to  $40\pm10\,\mathrm{nm}$  and to  $81\pm16\,\mathrm{nm}$ , compared with citrate stabilized AgNP:  $19\pm4\,\mathrm{nm}$  and  $58\pm10\,\mathrm{nm}$ , respectively (Fig. 1). This change results from the size of modifier ligand adsorbed on the surface of AgNP. The PEG-ligand (Mw=6000 g mol^-1) is much larger compared with citrate molecules. Hence, the hydrodynamic sizes of AgNP modified with PEG-ligand were larger than the hydrodynamic size of AgNP modified with citrate. The maxima of the adsorption band were

Table 1 Mean size and PDI of particles in suspensions containing silver nanoparticles (15 or 45 nm, at 470 μg/ml) stabilized with citrate or PEG, and AlCl $_3$  (500 μM), MPB (1250 μM), DBPH (35 μM). DLS measurements (size by intensity in nm and polydispersity index PDI) were performed after 24h of incubation at 37 °C. The measurements from 3 independent measurements repeated three times.

	After 24 h	
	Size by intensity (nm)	PDI
Citrate stabilized Ag 15 nm	36 ± 19 (96%)	$0.33 \pm 0.03$
+AlCl <sub>3</sub>	$34 \pm 19 \ (100\%)$	$0.12 \pm 0.02$
+MPB	$37 \pm 19 (94\%)$	$0.37 \pm 0.03$
+DBPH	$39 \pm 22 \ (95\%)$	$\textbf{0.35} \pm \textbf{0.01}$
Citrate stabilized Ag 45 nm	54 ± 17 (100%)	$0.14 \pm 0.01$
+AlCI <sub>3</sub>	$59 \pm 23 \ (100\%)$	$0.19 \pm 0.01$
+MPB	$56 \pm 18 \ (100\%)$	$0.15 \pm 0.01$
+DBPH	$55 \pm 17 \ (100\%)$	$\textbf{0.14} \pm \textbf{0.01}$
PEG stabilized Ag 15 nm	38 ± 12 (100%)	$0.08 \pm 0.01$
+AICl <sub>3</sub>	$31 \pm 4 (100\%)$	$0.19 \pm 0.06$
+MPB	$36 \pm 10 \ (100\%)$	$0.07 \pm 0.01$
+DBPH	$43 \pm 16 \ (98\%)$	$0.18 \pm 0.02$
PEG stabilized Ag 45 nm	78 ± 26 (100%)	$0.13 \pm 0.01$
+AlCl <sub>3</sub>	$72 \pm 22 \ (100\%)$	$0.11 \pm 0.01$
+MPB	$77 \pm 24 \ (100\%)$	$0.12 \pm 0.01$
+DBPH	$77 \pm 25 (100\%)$	$0.12 \pm 0.01$

recorded in the region characteristic for AgNP of a given size: at 411 nm and 435 nm for PEG stabilized Ag 15 nm and PEG stabilized Ag 45 nm, respectively.

DLS measurements of suspensions of AgNP in combinations with AlCl<sub>3</sub>, MPB or DBPH before and after 24h of incubation showed their good stability, suitable for skin absorption studies (Table 1).

#### 3.2. Validation of the biological system

Skin sections used for the studies obtained using dermatome showed uniform thickness (390  $\pm$  15  $\mu m,$  N = 10) that was reflected by the measurements in histopathological sections (Fig. 3A). MTT test performed immediately after thawing the skin and after 24 h of its incubation in the Franz chamber indicated that the disks retained quite significant capability for metabolic conversion of MTT (Fig. 3B).

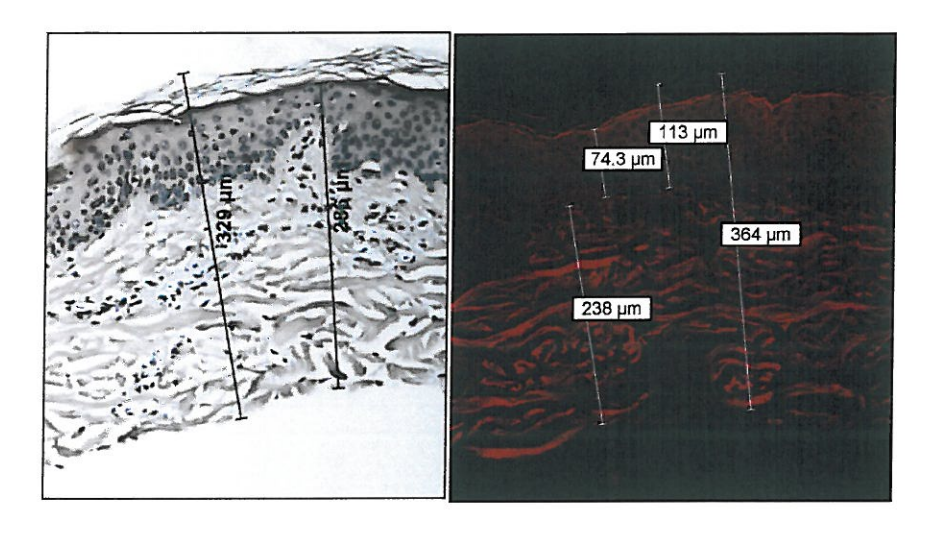
#### 3.3. Transdermal absorption of sliver

The measurements did not show any statistically significant differences in silver penetration between the 4 types of silver nanoparticles studied (15 and 45 nm AgNP, citrate or PEG stabilized) at 3 different concentrations, i.e. 47, 470 or 750  $\mu$ g/ml (Fig. 4). Although the values observed for citrate stabilized 45 nm AgNP tended to be lower compared to 15 nm AgNP, the difference was not significant. The medians for the 45 nm AgNP in combination with AlCl<sub>3</sub>, MPB or DBPH (Fig. 5) were slightly lower in comparison to the 15 nm AgNP in combination with the chemicals, in cases of both AgNP types, i.e. citrate (Ag45, 115–250 pg/cm² vs. Ag15, 295–385 pg/cm²) and especially PEG stabilized (90–178 pg/cm² vs. 313–448 pg/cm²). The differences, however, did not reach statistical significance.

Overall, the results indicate a very low penetration of silver through the skin, as generally only a very small fraction of the silver applied in the donor chamber (i.e. 75 µg for the highest concentration of 750 µg/ml) was detected in the receptor fluid (the measured highest amount of Ag that penetrated was 0.45 ng/cm² with range of 0.365–0.974 ng/cm² for PEG stabilized Ag15 + MPB). Moreover, the selected cosmetic ingredients did not have a statistically significant influence on the silver absorption.

Assessment of the skin sections morphology after 24 h exposure to AgNP at 3 concentrations as well as to the combinations of AgNP with the chemicals did not show any visible structural alterations (Fig. 6).





Disk 1. MTT test with В fresh (not frozen) skin sample

 $OD = 2.153 \pm 0.37$ 

Disk 2. MTT test immediately after thawing



 $OD = 1.432 \pm 0.16$ 

(67% fresh skin)

Disk 3. After 24 h incubation in Franz chamber, not trimmed, not incubated with MTT



incubation in Franz chamber, trimmed and incubated with MTT

Disk 4. After 24 h



 $OD = 0.892 \pm 0.16$ 

(41% fresh skin)

Fig. 3. Validation of the biological test system. A. Exemplary image with measurements of a split-thickness skin disk section stained using standard hematoxylin-eosin method or with Nile Red (fluorescence). B. Measurements of viability of pig skin disks in MTT reduction test. The disk 1: the skin was not frozen; exemplary disk prepared within 4 h after killing an animal was trimmed and incubated with MTT solution (0.5 mg/ml) for 3 h; the disk 2: exemplary skin disk prepared immediately after thawing; the disk 4: the skin after thawing was incubated in the Franz chamber for 24 h and thereafter was incubated with the MTT solution for 3 h. The samples were in triplicates and the results of optical density (OD) measurements are mean ± SD from 3 independent experiments.

#### 3.4. Analysis by laser ablation inductively coupled plasma mass spectrometry (LA-ICP-MS)

In spite of extensive washing of the skin disks after the exposure, and further preparation procedures including washing steps in inorganic and organic solvents, rather strong Ag signals could be seen at the top layers of the epidermis (Fig. 7). The presence of the signals might result from the AgNP residues bound to corneal layer or Ag which penetrated to superficial epidermal layers. A definitive answer to this question cannot be given because of low magnification of the CCD camera not permitting precise distinction of structural layers. However, in some sections clear Ag signals could be detected which were localized to hair follicles or even superficial dermal layers (e.g. Fig. 7. CIT 45, 750 ppm AgNP). In other sections a weak diffuse pattern of Ag signals could be observed without any gradient of intensity, particularly in the perpendicular plane. A quantitative visualization of the Ag signal maps of all skin sections analyzed is provided in Fig. 8. No clear pattern of a relationship between AgNP applied at different concentrations or AgNP in combination with the chemicals and silver percutaneous absorption could be seen.

#### 4. Discussion

In this study we conducted a series of experiments to determine if AlCl<sub>3</sub>, methyl paraben or butyl phthalate can modulate percutaneous absorption of AgNP. To the best of our knowledge this is the first study of such kind.

The DLS measurements performed after 24h of incubation of the AgNP in the presence of the chemicals confirmed good stability of the colloids. The unfrozen samples of pig skin used in our studies retained considerable metabolic capability. The results with MTT reduction test were fully compatible with available data. Cryopreserved Bama miniature pig skin was shown to maintain a level of skin metabolism equal to 77% of the fresh sample when measured immediately after thawing, and the viability remained about 30% after 24h at 25°C in DMEM (Ge et al., 2010). Similarly, Castagnoli et al. (2003) observed that the viability of thawed human allografts, cryopreserved with DMSO, and stored at 4°C, analyzed with MTT was about 54% of the "fresh" skin samples (the value obtained before cryopreserving treatment), which was 32% after 24h and 23% after 48h of storing at 4°C. Based on the histopathological examination, neither the AgNP at high

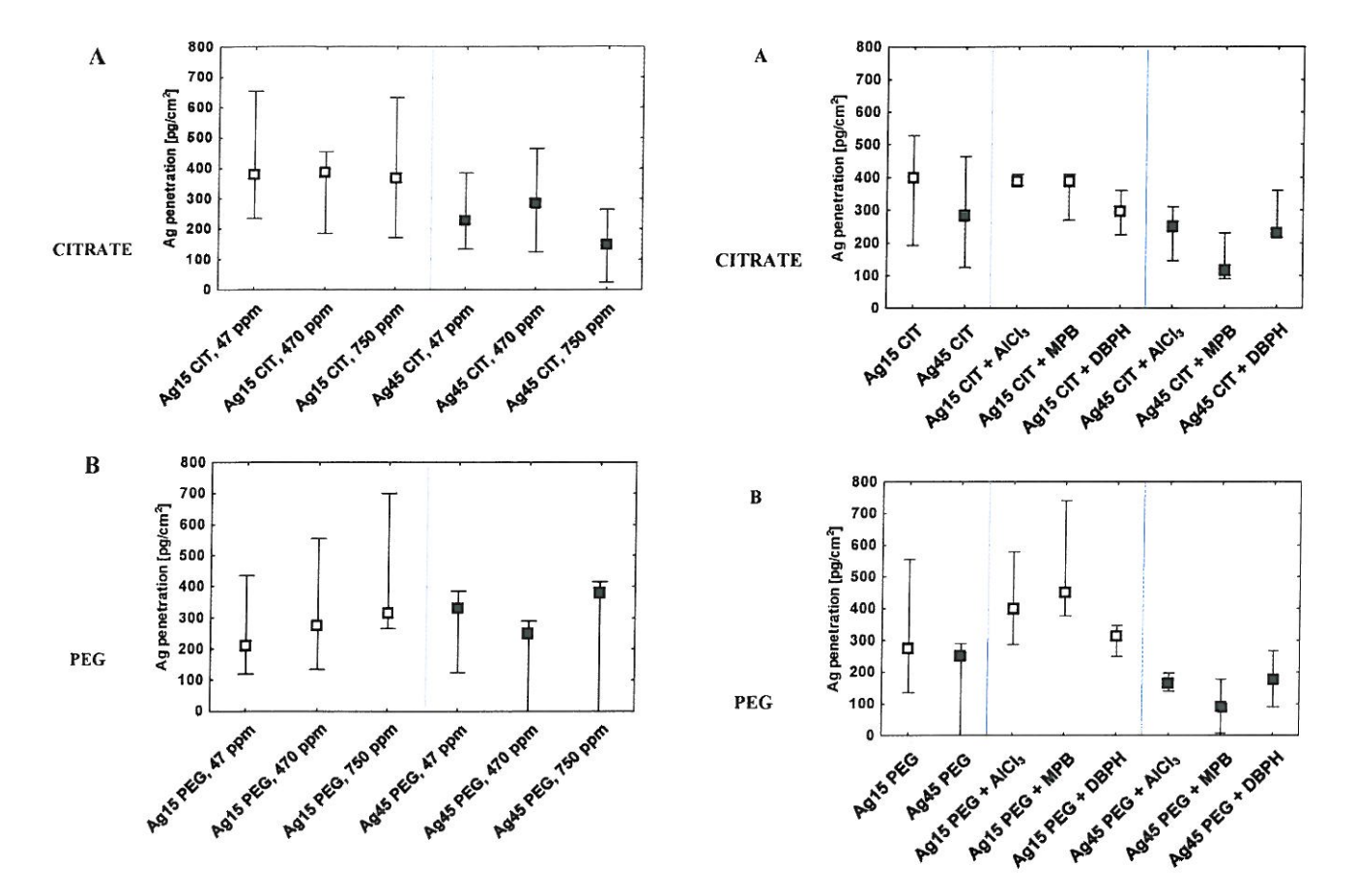


Fig. 4. Transdermal absorption of silver through the pig skin disks. Silver concentration was measured in the receptor fluid after 24h of incubation of the disks in static diffusion Franz chambers with: A. Citrate stabilized silver nanoparticles (Ag15 CIT and Ag45 CIT, both at 47, 470 or 750  $\mu$ g/ml) and B. PEG stabilized silver nanoparticles (Ag15 PEG and Ag45 PEG, both at 47, 470 or 750  $\mu$ g/ml). The skin samples were in triplicates and the results are medians (pg/cm²) with interquartile range from two independent experiments.

concentrations (up to 750 µg/ml) nor the 3 chemicals used at the highest achievable concentrations in aqueous solvent induced any discernible structural alterations in the skin. This examination further confirmed validity of our studies. Available experimental data with silver in nanosized or ionic form clearly indicates that it can have a toxic effect on cultured cells (with silver ions inducing generally higher toxicity) (Holmes et al., 2016; Galandáková et al., 2016), while exerting negligible or no toxic effects on normal skin using both in vitro (Kim et al., 2016) and in vivo models (Maneewattanapinyo et al., 2011; Korani et al., 2011).

Although the concentrations used of all test substances were generally high, most probably not encountered in real life conditions, it was our intention to follow such an exaggerated scenario. For comparison, the amount of silver released by a commercially available nanocrystalline silver dressing can be on the order of  $4.7\pm1.9~\mu g/ml$  (Bianco et al., 2015) or even  $70~\mu g/ml$  of silver ions (Ag\*) (Wright et al., 1998) (the lowest concentration used in our study was  $47~\mu g/ml$ ). It has to be realized that skin (and particularly, of the underarm region) can be exposed to unpredictably high concentrations of the chemicals caused by multiple application of the cosmetics often on regularly shaved surface (hence being impaired somehow). The local temperature, high humidity and increased density of hair follicles can all favor the increased rate of percutaneous absorption of particular chemicals.

**Fig. 5.** Transdermal absorption of silver through the pig skin disks. Silver concentration was measured in the receptor fluid after 24 h of incubation of the disks in static diffusion Franz chambers with: A. Citrate stabilized silver nanoparticles (Ag15 CIT or Ag45 CIT, both at 470  $\mu g/ml$ ) alone or with AlCl $_3$  (500  $\mu$ M), methyl paraben (MPB at 1250  $\mu$ M) or dibutyl phthalate (DBPH at 35  $\mu$ M) and B. PEG stabilized silver nanoparticles (Ag15 PEG or Ag45 PEG, both at 470  $\mu g/ml$ ) alone or with AlCl $_3$ , MPB or DBPH. The skin samples were in triplicates and the results are medians (pg/cm²) with interquartile range from one or two independent experiments.

There are few papers published on percutaneous absorption of silver nanoparticles, all of which indicate generally very low skin penetration rate of silver. However, it is suggested that this penetration can increase in cases of inflammatory diseases, structural defects of the barrier (e.g. in response to excessive sunlight exposure), wounds, etc. (Moiemen et al., 2011; Wang et al., 2009; Vlachou et al., 2007).

In our study we observed a very low but detectable fraction of silver absorbed through the skin disks. The absorption did not depend on concentration, or the size and stabilization mode of the nanoparticles. The highest median penetration measured was 0.45 ng/cm². Our results are similar to those reported by Larese et al. (2009), who found median silver penetration of 0.46 ng/cm² for polyvinylpirrolidone-stabilized silver nanoparticles (25  $\pm$  7.1 nm by TEM) applied on intact human skin for 24 h. Bianco et al. (2014) reported an order of magnitude higher 24 h silver penetration of 4.8 ng/cm² for fresh human skin and 7.2 ng/cm² for cryopreserved human skin (PVP-stabilized silver nanoparticles, size of  $19\pm5$  nm).

The mechanisms of AgNP skin penetration are not clearly understood. Theoretically 2 major routes for the penetration may

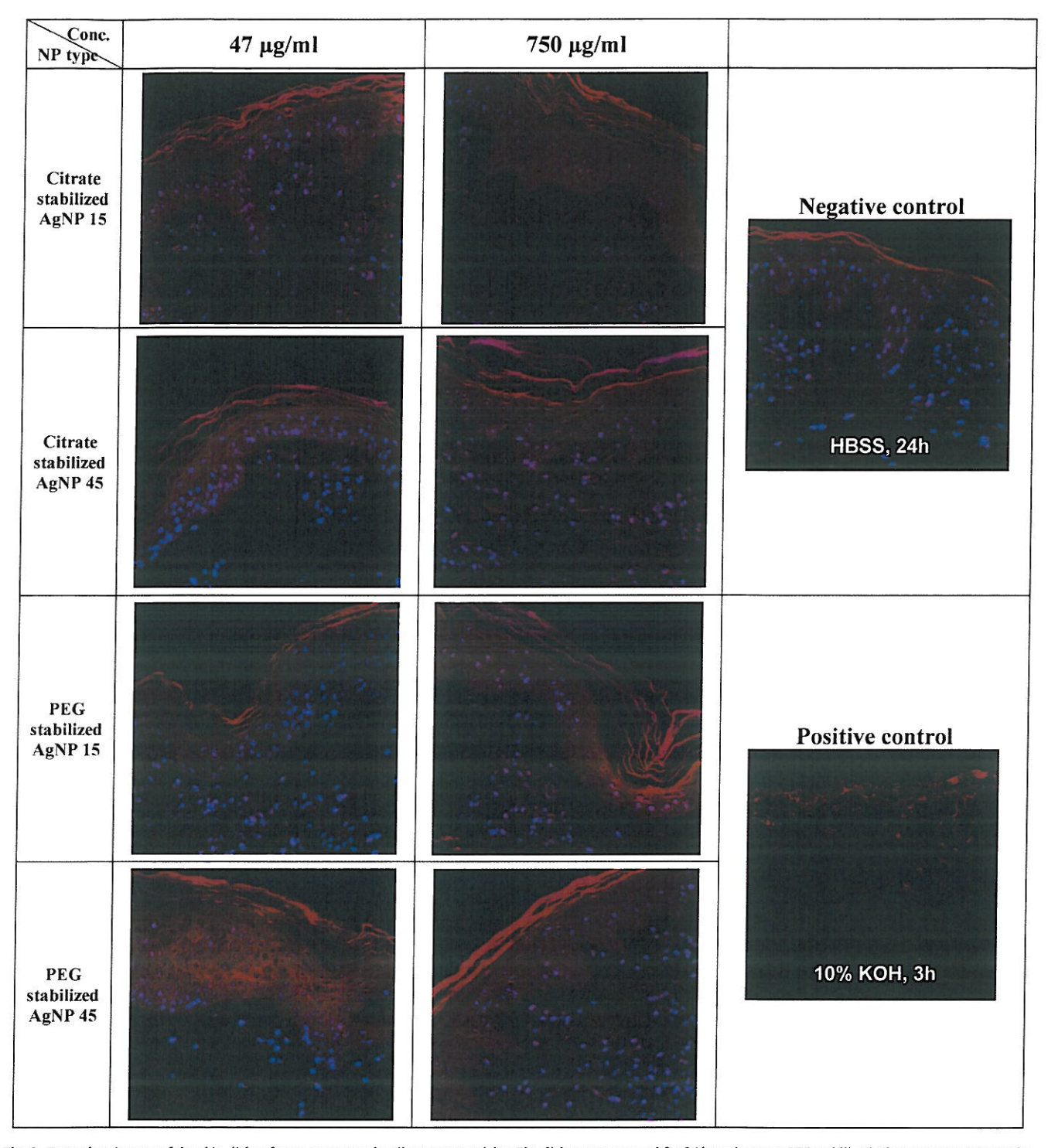


Fig. 6. Exemplary images of the skin disks after exposure to the silver nanoparticles. The disks were exposed for 24 h to citrate or PEG stabilized silver nanoparticles at the lowest (47 μg/ml) or the highest (750 μg/ml) concentrations. All sections show normal structures. For comparison disks treated with HBSS only (negative control) or 10% KOH for 3 h are shown. The sections were stained with Nile Red and DAPI.

exist: across the stratum corneum, by an intercellular or transcellular route, and through skin appendages (i.e. hair follicles and sweat glands). Although the width of follicle infundibula can be micrometers in size, it has been reported that only 40 nm nanoparticles penetrated into hair openings and through the follicular epithelium, and that larger particles (750 and 1500 nm) became lodged at the hair follicle infundibulum (Vogt et al., 2006).

Some studies suggest that silver penetration through the skin can rely on the mechanism of passive diffusion (Bianco et al., 2014). Other data indicates dependence of the penetration on the shape of the silver nanoparticles. Rod-shape AgNP penetrated the dermal layer at a depth of 244  $\mu$ m, in contrast to triangular or sphere shape AgNP, which were detected in the stratum corneum at the depth of approximately 10  $\mu$ m, or in epidermal layer at a depth of 14.9–

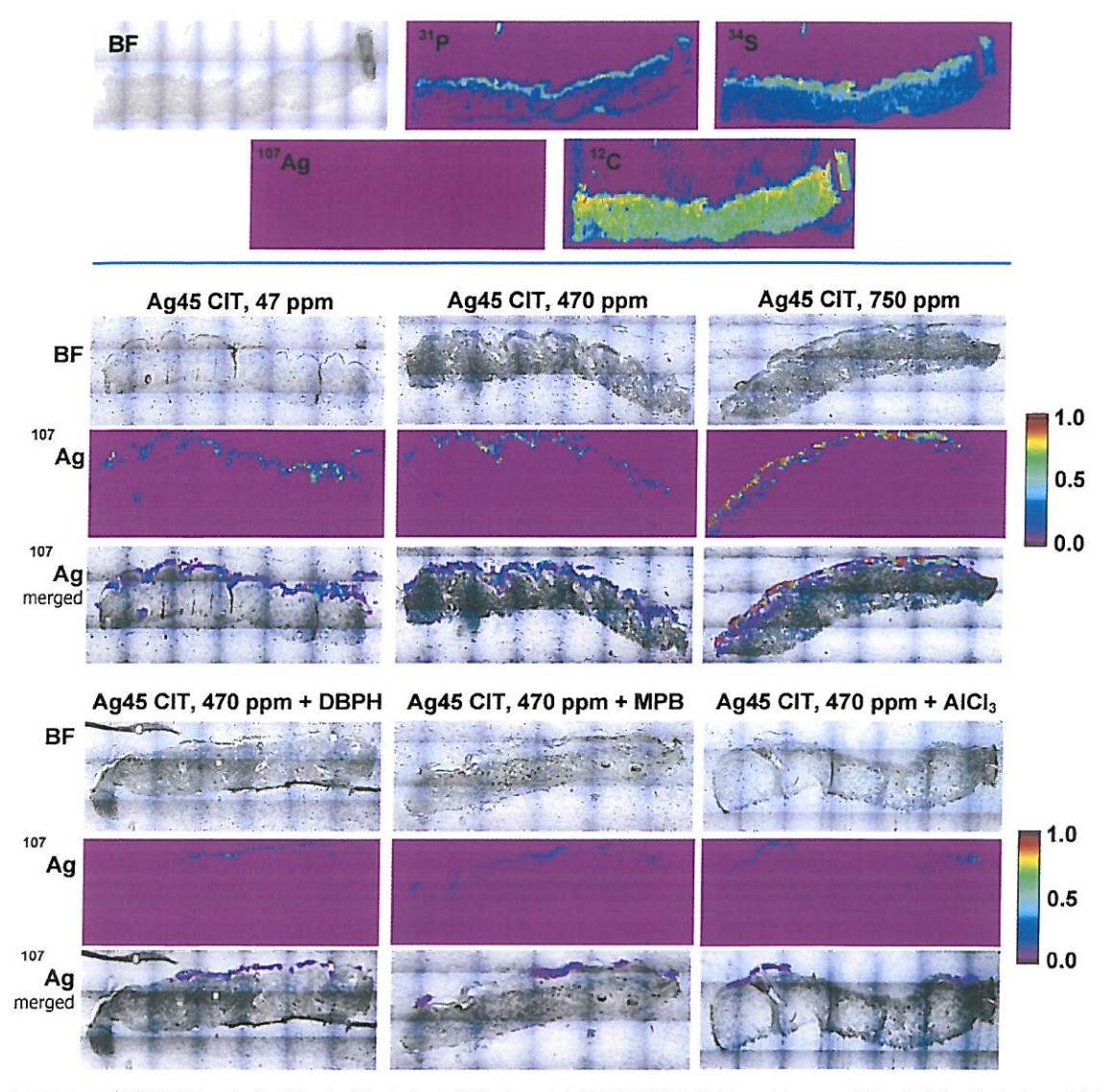


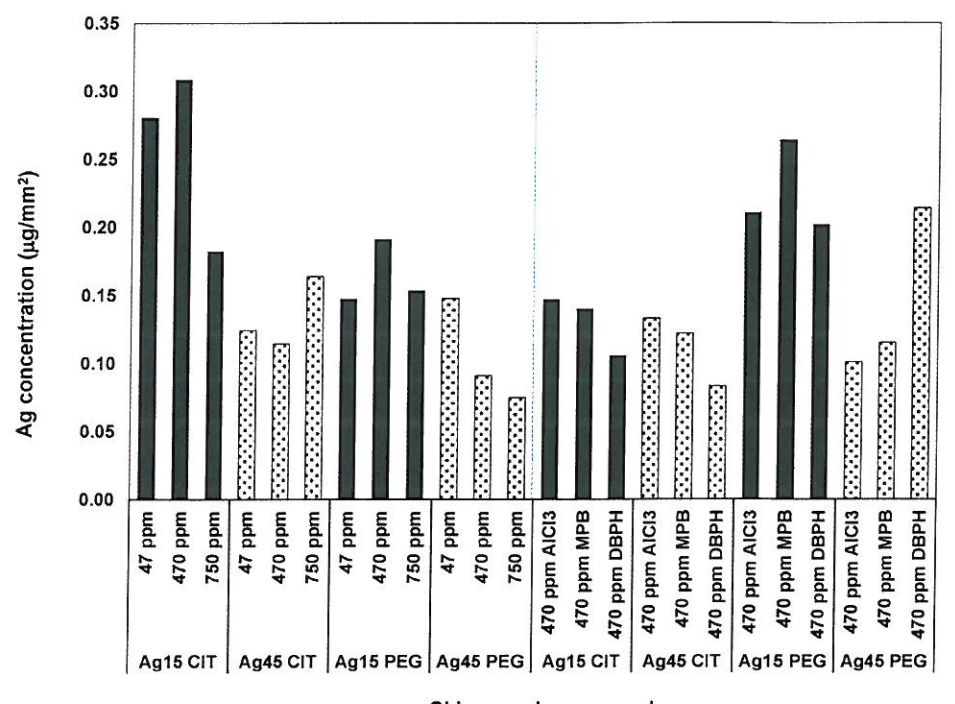
Fig. 7. Exemplary images of LA-ICP-MS analysis of the pig skin sections. At the top – bright field (BF) digital camera images of the pig skin prior to laser ablation and the elemental maps of phosphorus, sulfur, carbon and silver. For carbon, the surrounding paraffin signal which was much lower than for the tissue, was subtracted out. Below – the Ag elemental maps display the accumulation of Ag. The skin disks were exposed for 24 h to 3 concentrations of citrate stabilized AgNP 45 nm at 3 concentrations (the upper panel) or to AgNP 45 nm at 470 ppm in combination with DBPH (35 μM), MPB (1250 μM) or AlCl<sub>3</sub> (500 μM) (the lower panel).

19.9  $\mu$ m, respectively (Tak et al., 2015). Interestingly, in mice topical application of the rod-shape AgNP led to the highest silver concentration in blood (108 ng/mL), while concentration of silver permeated from sphere or triangular AgNP in blood were 50 ng/mL and 39 ng/mL, respectively. George et al. (2014) suggested a possibility that Ag $^{+}$  ions can penetrate individually and reaggregate again in the dermis or form inorganic silver species, e.g. Ag $_{2}$ S or other compounds.

In our study we did not observe any statistical differences in percutaneous absorption between the AgNP, irrespective of their size, surface modification, or co-presence of the test chemicals. However, slightly lower values of silver penetration could be noticed for the bigger AgNP in combination with the test chemicals. In the open literature we could not find any relevant data on percutaneous absorption of AgNP in relation to their different size or surface modification. Similarly, no data exists on the absorption of AgNP when combined with other chemicals, in spite the fact that in majority of skin formulations AgNP are used in complex mixtures of chemicals. It is commonly known that in

biological fluids containing proteins, nanoparticles including AgNP, are quickly coated with protein corona, suggested to be more significant in determining the biological response than the bare material properties of the particle itself. The parameters that may affect corona composition include particle size, particle shape and particle surface properties as well as biological fluid properties and composition (Durán et al., 2015b). Although, in our study any potential influence of protein corona on AgNP absorption can be excluded (because of using HBSS without proteins), interactions of the nanoparticles with the test chemicals, particularly with aluminum, are probable, but currently unknown. In any case, the chemicals did not increase the skin penetration of AgNP, irrespective of their size or surface modification.

Imaging of metals in tissue sections by laser ablation inductively coupled plasma mass spectrometry (LA-ICP-MS) is a powerful technique for profiling of elements (Becker et al., 2014). In our study we used this technique to map whole skin cross-sections prepared after exposure to all four types of silver nanoparticles, also in combinations with the selected chemicals.



## Skin samples exposed

Fig. 8. Amount of silver detected in each skin sample tested. The skin disks were exposed for 24 h to 3 concentrations of citrate or PEG stabilized AgNP 45 nm or AgNP 15 nm (47, 470 or 750  $\mu$ g/ml) or to all four AgNP at 470  $\mu$ g/ml in combination with AlCl<sub>3</sub> (at 500  $\mu$ M), methyl paraben (MPB at 1250  $\mu$ M) or dibutyl phthalate (DBPH at 35  $\mu$ M) (N = 1). The results of LA-ICP-MS measurements are expressed in  $\mu$ g Ag/mm<sup>2</sup>.

Although there are other sensitive microanalytical element imaging techniques available (e.g. X-ray spectroscopic techniques and secondary ion mass spectrometry (SIMS)), LA-ICP-MS offers the lowest limits of detection at the µg/g range and below (Becker et al., 2014). The LA technique works by firing the laser at a fixed spot size of 35 µm and a stage speed of 0.1 mm/s, in such that the biological material is ablated (total consumption of the tissue) in a raster motion. During the ablation process each laser pulse removes the material, a small plasma is created, and during the cooling of this plasma nanoparticles are formed. These nanoparticles are then swept into an ICP torch using helium gas. Once the particles are introduced into the ICP plasma, they are vaporized, atomized, and excited/ionized. The isotopes of interest are collected in a time resolved manner and using Applied Spectra's Data Analysis software high resolution 2D elemental images were created for each skin tissue sample analyzed. Unfortunately, the measurements did not provide clear proof for silver penetration through the skin samples. We expected to observe silver distribution across the section in a form of a gradient of signal intensity; however, none of the elemental maps demonstrated such a distribution. Instead we observed minute amounts of silver nanoparticles deposited in hair follicle appendices (some maps clearly indicated this possibility) which then could diffuse into receptor fluid likely in the form of silver ions. There is also possibility that a fraction of the silver which penetrated into skin was solubilized in aqueous solvents during fixation (10% formalin) or preparation of the sections (dehydration in ethanol). Nevertheless, these procedures did not result in a complete dissolution of silver nanoparticles from the sections, and in almost all of them strong signals could be detected at the stratum

In conclusion, our results do not indicate any influence of aluminum chloride, methyl paraben or dibutyl phthalate on silver nanoparticles penetration rate through the pig skin. Although we used aqueous environment not ideally reflecting the mode of skin cosmetics application, we believe that such studies on biological effects of silver nanoparticles in complex mixtures with chemicals in standard form provide new valuable data on potential toxic mechanisms.

#### Acknowledgements

The study was funded by the Polish National Science Centre (Grant 2012/07/B/NZ7/04197). The part of the study has been carried out on the apparatus purchased in projects: POIG.01.03.01-00-004/08 Functional nano- and micro textile materials – NANO-MITEX co-financed by the European Union with the financial resources of the European Regional Development Fund and the National Centre for Research and Development.

#### Appendix A. Supplementary data

Supplementary data associated with this article can be found, in the online version, at http://dx.doi.org/10.1016/j.toxlet.2017.03.006.

#### References

Becker, J.S., Matusch, A., Wu, B., 2014. Bioimaging mass spectrometry of trace elements – recent advance and applications of LA-ICP-MS: a review. Anal. Chim. Acta 835 (2014), 1–18.

Bianco, C., Adami, G., Crosera, M., Larese, F., Casarin, S., Castagnoli, C., Stella, M., Maina, G., 2014. Silver percutaneous absorption after exposure to silver nanoparticles: a comparison study of three human skin graft samples used for clinical applications. Burns 40, 1390–1396.

Bianco, C., Kezic, S., Crosera, M., Svetličić, V., Šegota, S., Maina, G., Romano, C., Larese, F., Adami, G., 2015. In vitro percutaneous penetration and characterization of silver from silver-containing textiles. Int. J. Nanomed. 10, 1899–1908.

Castagnoli, C., Alotto, D., Cambieri, I., Casimiri, R., Aluffi, M., Stella, M., Alasia, S.T., Magliacani, G., 2003. Evaluation of donor skin viability: fresh and cryopreserved skin using tetrazolium salt assay. Burns 29, 759–767.

- Durán, N., Durán, M., de Jesus, M.B., Seabra, A.B., Fávaro, W.J., Nakazato, G., 2015a. Silver nanoparticles: a new view on mechanistic aspects on antimicrobial activity. Nanomedicine doi:http://dx.doi.org/10.1016/j.nano.2015.11.016 2015 Dec 24. pii: S1549-9634(15)00600-0. [Epub ahead of print],
- Durán, N., Silveira, C.P., Durán, M., Martinez, D.S.T., 2015b. Silver nanoparticle protein corona and toxicity: a mini-review. J. Nanobiotechnol. 13, 55
- Galandáková, A., Franková, J., Ambrožová, N., Habartová, K., Pivodová, V., Zálešák, B., Šafářová, K., Smékalová, M., Ulrichová, J., 2016. Effects of silver nanoparticles on human dermal fibroblasts and epidermal keratinocytes. Hum. Exp. Toxicol. 35, 946-957
- Ge, L., Sun, L., Chen, J., Mao, X., Kong, Y., Xiong, F., Wu, J., Wei, H., 2010. The viability change of pigskin in vitro. Burns 36, 533–538.
- George, R., Merten, S., Wang, T.T., Kennedy, P., Maitz, P., 2014. In vivo analysis of dermal and systemic absorption of silver nanoparticles through healthy human skin. Australas. J. Dermatol. 55, 185-190.
- Holmes, A.M., Lim, J., Studier, H., Roberts, M.S., 2016. Varying the morphology of silver nanoparticles results in differential toxicity against micro-organisms. HaCaT keratinocytes and affects skin deposition. Nanotoxicology 10, 1503-1514.
- Kim, H., Choi, J., Lee, H., Park, J., Yoon, B.I., Jin, S.M., Park, K., 2016. Skin corrosion and irritation test of nanoparticles using reconstructed three-dimensional human skin model, EpiDerm<sup>™</sup>. Toxicol. Res. 32, 311–316.
  Koniecki, D., Wang, R., Moody, R.P., Zhu, J., 2011. Phthalates in cosmetic and personal
- care products: concentrations and possible dermal exposure. Environ. Res. 111, 329-336.
- Korani, M., Rezayat, S.M., Gilani, K., Arbabi Bidgoli, S., Adeli, S., 2011. Acute and subchronic dermal toxicity of nanosilver in guinea pig. Int. J. Nanomed. 6, 855-
- Larese, F.F., D'Agostin, F., Crosera, M., Adami, G., Renzi, N., Bovenzi, M., Maina, G., 2009. Human skin penetration of silver nanoparticles through intact and damaged skin. Toxicology 255, 33-37.
- Maneewattanapinyo, P., Banlunara, W., Thammacharoen, C., Ekgasit, S. Kaewamatawong, T., 2011. An evaluation of acute toxicity of colloidal silver nanoparticles. J. Vet. Med. Sci. 73, 1417-1423.
- Moiemen, N.S., Shale, E., Drysdale, K.J., Smith, G., Wilson, Y.T., Papini, R., 2011.
- Acticoat dressings and major burns: systemic silver absorption. Burns 37, 27–35. Monteiro-Riviere, N.A., Riviere, J., 1996. The pig as a model for cutaneous pharmacology and toxicology research. In: Thmbleson, M.E., Schook, L.B. (Eds.), Advances in Swine in Biomedical Research. Proceedings of an International Symposium on Swine in Biomedical Research, held October 22-25, 1995, at the University of Maryland, University College Park, Maryland, Springer Science + Business Media New York, pp. 425–458.
  Pfurtscheller, K., Petnehazy, T., Goessler, W., Bubalo, V., Kamolz, L.P., Trop, M., 2014.
- Transdermal uptake and organ distribution of silver from two different wound dressings in rats after a burn trauma. Wound Repair Regen. 22, 654-659.

- Rouse, J.G., Yang, J., Ryman-Rasmussen, J.P., Barron, A.R., Monteiro-Riviere, N.A. 2007. Effects of mechanical flexion on the penetration of fullerene amino acidderivatized peptide nanoparticles through skin. Nano Lett. 7, 155–160.
- Scientific Committee on Consumer Products, 2007. SCCP/1016/06. Opinion on Phthalates in Cosmetic Products. Adopted by the SCCP at its 11th Plenary Meeting of 21 March.
- Scientific Committee on Consumer Safety, 2010. SCCS/1348/10. Opinion on Parabens. Adopted by the SCCS at its 9th Plenary on 14 December.
- Scientific Committee on Consumer Safety, 2013. SCCS/1514/13. Opinion on Parabens, Updated Request for a Scientific Opinion on Propyl- and Butylparaben, Adopted by the SCCS by Written Procedure on 3 May.
- Soni, M.G., Taylor, S.L., Greenberg, N.A., Burdock, G.A., 2002. Evaluation of the health aspects of methyl paraben: a review of the published literature. Food Chem. Toxicol. 40, 1335-1373.
- Tak, Y.K., Pal, S., Naoghare, P.K., Rangasamy, S., Song, J.M., 2015. Shape-dependent skin penetration of silver nanoparticles: does it really matter? Sci. Rep. 5, 16908. Vance, M.E., Kuiken, T., Vejerano, E.P., McGinnis, S.P., Hochella Jr., M.F., Rejeski, D.,
- Hull, M.S., 2015. Nanotechnology in the real world: redeveloping the nanomaterial consumer products inventory. Beilstein J. Nanotechnol. 6, 1769-
- Vlachou, E., Chipp, E., Shale, E., Wilson, Y.T., Papini, R., Moiemen, N.S., 2007. The safety of nanocrystalline silver dressings on burns: a study of systemic silver absorption. Burns 33, 979-985.
- Vogt, A., Combadiere, B., Hadam, S., Stieler, K.M., Lademann, J., Schaefer, H., Autran, B., Sterry, W., Blume-Peytavi, U., 2006. 40 nm, but not 750 or 1,500 nm, nanoparticles enter epidermal CD1a+ cells after transcutaneous application on human skin. J. Invest. Dermatol. 126, 1316–1322. Wang, X.Q., Kempf, M., Mott, J., Chang, H.E., Francis, R., Liu, P.Y., Cuttle, L., Olszowy,
- H., Kraychuk, O., Mill, J., Kimble, R., 2009. Silver absorption on burns after the application of Acticoat<sup>TM</sup>: data from pediatric patients and a porcine burn model. J. Burn Care Res. 30, 341–348.
- Wright, J.B., Hansen, D.L., Burrell, R.E., 1998. The comparative efficacy of two antimicrobial barrier dressings: in-vitro examination of two controlled release of silver dressings. Wounds 10, 179–188. Zhang, L.W., Monteiro-Riviere, N.A., 2008. Assessment of quantum dot penetration
- into intact, tape-stripped, abraded and flexed rat skin. Skin Pharmacol. Physiol.
- Zhu, Y., Choe, C.S., Ahlberg, S., Meinke, M.C., Alexiev, U., Lademann, J., Darvin, M.E., 2015. Penetration of silver nanoparticles into porcine skin ex vivo using fluorescence lifetime imaging microscopy, Raman microscopy, and surfaceenhanced Raman scattering microscopy. J. Biomed. Opt. 20, 051006.